Self-Assembly of β-Sheets into Nanostructures by Poly(alanine) Segments Incorporated in Multiblock Copolymers Inspired by Spider Silk

Osman Rathore and Dotsevi Y. Sogah*

Contribution from the Department of Chemistry and Chemical Biology, Cornell University, Baker Laboratory, Ithaca, New York 14853-1301

Received November 20, 2000

Abstract: Selective replacement of the amorphous peptide domain of a spider silk with poly(ethylene glycol) gave *N. clavipes* silk-inspired polymers having similar solid-state structures and very good mechanical properties. The tendency of poly(alanine) having appropriate chain length to form β-sheets and the facility with which the β-sheets self-assemble have been retained in the polymers. Solid-state ^{13}C NMR, solid-state FTIR, X-ray diffraction, and AFM studies showed that the polymers formed predominantly antiparallel β-sheets that self-assembled into discrete nanostructures. The longer the peptide segment was, the greater was the tendency to self-assemble into antiparallel β-sheet aggregates. AFM revealed that the morphology of the polymers was a microphase-separated architecture that contained irregularly shaped 100−200 nm poly(alanine) nanodomains interspersed within the PEG phase. The results suggest that the poly(alanine) domain influences the solid-state properties of spider silk through β-sheet self-assembly into temporary cross-links. The results further demonstrate that by selectively replacing certain segments of a naturally occurring biopolymer with a judiciously selected nonnative segment while, at the same time, retaining other segments known to be critical for the essential properties of the native biopolymer, a synthetic polymer with similar properties and function can be obtained.

Introduction

The ultimate goal in synthetic polymer chemistry is the precise control of molecular architecture, which has been the focus of intensive research for some time.[1] Notwithstanding the great strides made in structure control using living polymerizations[1a−f] and step-by-step construction of dendritic structures,[1g−k] precise polymer structure control has, for the most part, eluded polymer chemists. In contrast, the precise control of the architecture of biopolymers is routinely done by nature. Hence, biological systems represent a quintessential paradigm in biomimetic research directed to structure control, especially since their various components self-assemble into useful nanostructures with strong correlation between structure and function. Therefore the efforts of polymer chemists directed to precisely controlling polymer architecture and nanostructure formation in synthetic materials might benefit from the biochemical principles that govern secondary structure formation, predictable folding, and self-assembly in biopolymers.[2,3] A successful application of lessons learned from nature to polymer architecture control will, undoubtedly, have a significant impact on the design and production of novel biomaterials with applications in protein/cell immobilization, controlled drug delivery, biosensors, self-assembling electronic devices, and medical reconstruction devices.[4]

In the search for clues from nature one finds that there are many fibrous proteins with repetitive peptide sequences that fold into regular structural elements and define the properties of the biopolymer.[3,5] Examples include keratin,[3a] collagen,[3a] fibronectin,[3a] silks,[3c] elastin,[5a] and amelogenins.[5b,c] Examination of the

(1) (a) For detailed reviews, see: *Comprehensive Polymer Science. The Synthesis, Characterization, Reactions and Applications of Polymers*; Eastmond, G. C., Ledwith, A., Russo, S., Sigwalt, P., Eds.; Pergamon Press: New York, 1989; Vols. I−IV. (b) *Frontiers of Macromolecular Science*; Saegusa, T., Higashimura, T., Abe, A., Eds.; Blackwell Scientific Publications: Oxford, 1989. (c) Webster, O. W. *Science* **1991**, *251*, 887. (d) Hertler, W. R.; Webster, O. W.; Cohen, G. M.; Sogah, D. Y. *Macromolecules* **1987**, *20*, 1473−1488. (e) Rempp, P. F.; Lutz, P. J. In *Comprehensive Polymer Chemistry*; Allen, G., Ed.; Pergamon: Oxford, 1992, Chapter 12. (f) Rizzardo, E.; Chiefari, J.; Chong, B. Y. K.; Ercole, F.; Krstina, J.; Jeffery, J.; Le, T. P. T.; Mayadunne, R. T. A.; Meijs, G. F.; Moad, C. L.; Moad, G.; Thang, S. H. *Macromol. Symp.* **1999**, *143*, 291−307. (g) Hawker, C. J. *Adv. Polym. Sci.* **1999**, *147*, 113−160. (h) Frechet, J. M. J. *Science* **1994**, *263*, 1710−1715. (i) Newkome, G. R.; Baker, G. R.; Young, J. K.; Traynham, J. G. *J. Polym. Sci., Polym. Chem.* **1993**, *31*, 641. (j) Tomalia, D. A. *Adv. Mater.* **1994**, *6*, 529. (k) Sunder, A.; Mulhaupt, R.; Haag, R.; Frey, H. *Adv. Mater.* **2000**, *12*, 235−239.

(2) (a) Aggeli, A.; Bell, M.; Boden, N.; Harding, R.; McLeish, T. C. B.; Nykova, I.; Radford, S. E.; Semenov, A. *Biochemistry* **2000**, *22*, 10−14. (b) Barron, A. E.; Zuckermann, R. N. *Curr. Opin. Chem. Biol.* **1999**, *3*, 681−687. (c) Krejchi, M. T.; Atkins, E. D. T.; Waddon, A. J.; Fournier, M. J.; Mason, T. L.; Tirrell, D. A. *Science* **1994**, *265*, 1427. (d) Yu, S. M.; Soto, C. M.; Tirrell, D. A. *J. Am. Chem. Soc.* **2000**, *122*, 6552−6559. (e) McMillan, R. A.; Conticello, V. P. *Macromolecules* **2000**, *33*, 4809−4821. (f) Buchko, C. J.; Slattery, M. J.; Kozloff, K. M.; Martin, D. C. *J. Mater. Res.* **2000**, *15*, 231−242. (g) Kobatake, E.; Onoda, K.; Yanagida, Y.; Aizawa, M. *Biomacromolecules* **2000**, *1*, 382−386. (h) Heslot, H. *Biochimie* **1998**, *80*, 19−31. (i) McGrath, K. P.; Kaplan, D. L. *Macromol. Symp.* **1994**, *77*, 183−9. (j) Stupp, S. I.; LeBonheur, V.; Walker, K.; Li, L. S.; Huggins, K. E.; Keser, M.; Amstutz, A. *Science* **1997**, *276*, 384−389. (k) *Protein-Based Materials*; McGrath, K. P., Kaplan, D. L., Eds.; Birkhaeuser: Cambridge, MA, 1997. (l) Krejchi, M. T.; Cooper, S. J.; Deguchi, Y.; Atkins, E. D. T.; Fournier, M. J.; Mason, T. L.; Tirrell, D. A. *Macromolecules* **1997**, *30*, 5012. (m) McGrath, K. P.; Fournier, M. J.; Mason, T. L.; Tirrell, D. A. *J. Am. Chem. Soc.* **1992**, *114*, 727. (n) Sogah, D. Y.; Perle-Treves, D.; Voyer, N.; DeGrado, W. F. *Macromol. Symp.* **1994**, *88*, 149−163.

(3) (a) Fraser, R. D. B.; MacRae, T. P. *Conformation in Fibrous Proteins and Related Synthetic Polypeptides*; Academic Press: New York, 1973. (b) Fasman, G. D. In *Prediction of Protein Structure and the Principles of Protein Conformation*; Fasman, G. D., Ed.; Plenum Press: New York, 1989; pp 193−316. (c) *Silk Polymers: Materials Science and Biotechnology*; Kaplan, D., Adams, W. W., Farmer, B., Viney, C., Eds.; American Chemical Society: Washington, DC, 1994.

10.1021/ja004030d CCC: $20.00
Published on Web 05/12/2001

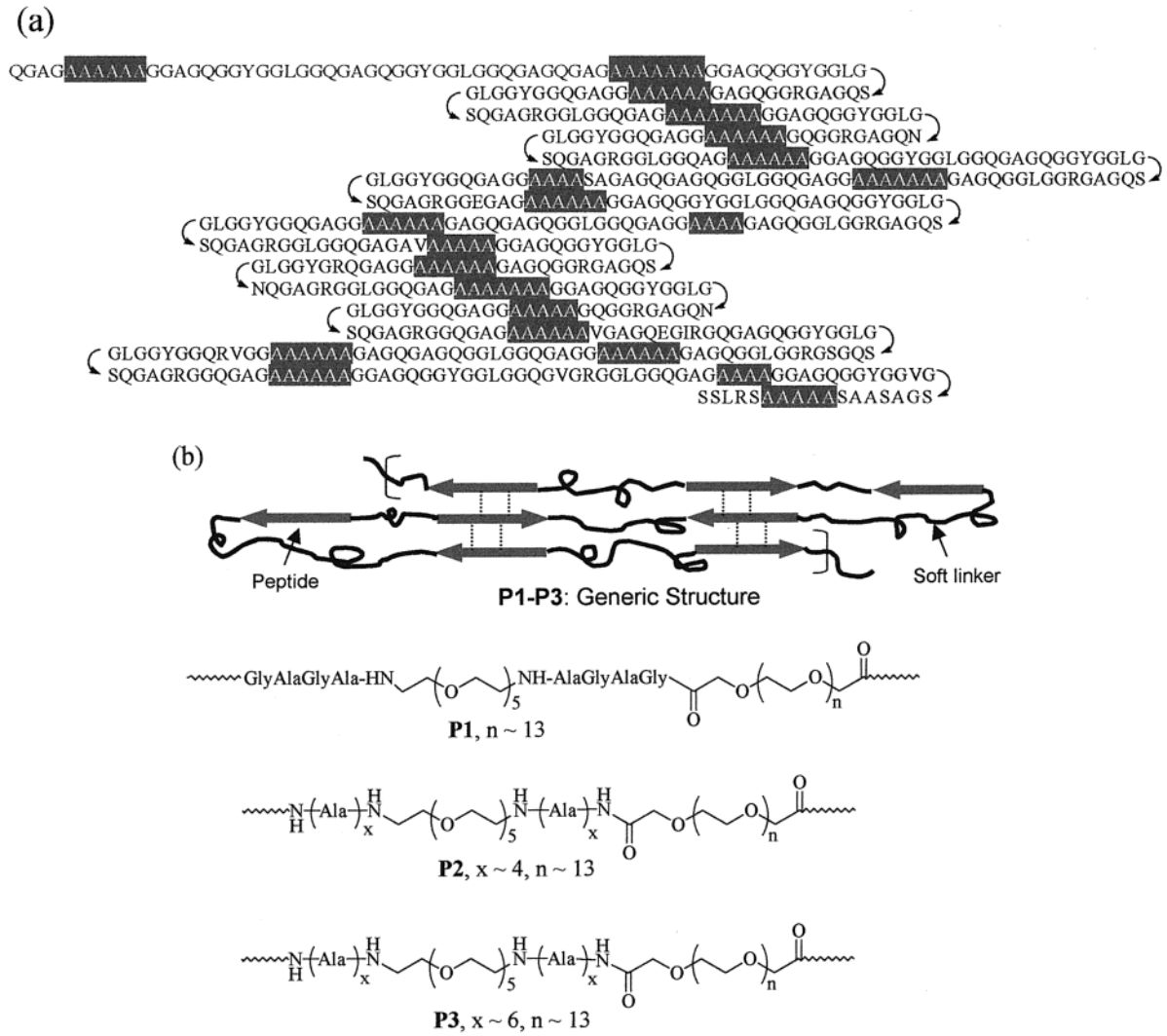

Figure 1. (a) *N. clavipes* major ampullate sequence showing the alanine-rich β-sheets (highlighted) and glycine-rich amorphous regions.[10] (b) Generic structure of designed silk-inspired segmented multiblock copolymers **P1**−**P3** in which the amorphous segments are replaced by flexible nonpeptide blocks.

structures of some of these biopolymers reveals that they resemble the structures of segmented multiblock copolymers. For example, naturally occurring silks consist of β-sheet crystalline segments (e.g., $(GlyAlaGlyAlaGlySer)_n$ for *Bombyx mori* silk or $(Ala)_n$ for *Nephila clavipes* silk) that alternate with amorphous segments composed of amino acids some of which have bulky side groups.[3c,6] This is illustrated in Figure 1a for one type of spider silk. Hence, properly designed segmented multiblock copolymers could help unlock the molecular secrets of structural biopolymers and provide the much-needed fundamental principles for the design and synthesis of polymers of controlled structures.

The structure and the excellent mechanical properties of natural silks have inspired several research laboratories to utilize lessons learned from nature in exploring the relationship between molecular structure and function.[2c,h,i,k−m,3c,6,7] Thus, genes coding for silk proteins in bacteria and yeast have yielded various silk analogues that have provided valuable clues. Fahnestock et al. have successfully expressed spider silk analogue proteins in *P. pastoris*.[7a] Kaplan et al. prepared high performance fibers based on *N. clavipes* dragline protein sequence.[7b] Similar approaches have resulted in a silk-like polymer containing a 17-residue fibronectin sequence as a cell adhesive

(4) (a) West, J. L.; Halas, N. J. *Curr. Opin. Biotechnol.* **2000**, *11*, 215−217. (b) Wooley, K. L. *J. Polym. Sci., Part A: Polym. Chem.* **2000**, *38*, 1397−1407. (c) Niemeyer, C. M.; Adler, M.; Pignataro, B.; Lenhert, S.; Gao, S.; Chi, L.; Fuchs, H.; Blohm, D. *Nucleic Acids Res.* **1999**, *27*, 4553−4561. (d) Niemeyer, C. M.; Burger, W.; Peplies, J. *Angew. Chem., Int. Ed. Engl.* **1998**, *37*, 2265−2268. (e) Petka, W. A.; Hardin, J. L.; McGrath, K. P.; Wirtz, D.; Tirrell, D. A. *Science* **1998**, *281*, 389−392. (f) McGrath, K. P.; Butler, M. M. In *Protein-Based Materials*; McGrath, K. P., Kaplan, D. L., Eds.; Birkhaeuser: Cambridge, MA, 1997; pp 251−279. (g) Pompe, W.; Mertig, M.; Kirsch, R. *Wiss. Z. Technol. University Dresden* **1997**, *46*, 40−45. (h) National Research Council Report: *Biomolecular Self-Assembling Materials: Scientific and Technological Frontiers*; National Academy Press: Washington, DC, 1996. (i) Safinya, C. R.; Shen, Y. *NATO ASI Ser. (E)* **1996**, *322*, 103−134. (j) Bayley, H. *J. Cell. Biochem.* **1994**, *56*, 168−70.

(5) (a) Urry, D. W. *J. Protein Chem.* **1988**, *7*, 1−34. (b) Aoba, T.; Moreno, E. C. In *Surface Active Peptides and Polymers*; Sikes, C. S., Wheeler, A. P., Eds.; American Chemical Society: Washington, DC, 1991, Chapter 7, pp 85−106. (c) Renugopalakrishnan, V.; Pattabiraman, N.; Prabhakaran, M.; Strawich, E. S.; Glimche, M. J. *Biopolymers* **1989**, *28*, 297.

(6) (a) Kaplan, D. L.; Mello, C. M.; Arcidiacono, S.; Fossey, S.; Senecal, K.; Muller, W. In *Protein-Based Materials*; McGrath, K. P., Kaplan, D. L., Eds.; Birkhaeuser: Cambridge, MA, 1997; pp 103−131. (b) Hayashi, C. Y.; Shipley, N. H.; Lewis, R. V. *Int. J. Biol. Macromol.* **1999**, *24*, 271−275. (c) Thiel, B. L.; Guess, K. B.; Viney, C. *Biopolymers* **1997**, *41*, 703−719.

(7) (a) Fahnestock, S. R.; Bedzyk, L. A. *Appl. Microbiol. Biotechnol.* **1997**, *47*, 33−39. (b) Prince, J. T.; McGrath, K. P.; DiGirolamo, C. M.; Kaplan, D. L. *Biochemistry* **1995**, *34*, 10879−10885. (c) Anderson, J. P.; Cappello, J.; Martin, D. C. *Biopolymers*, **1994**, *34*, 1049. (d) Cappello, J.; Crissman, J.; Dorman, M.; Mikolajczak, M.; Textor, G.; Marquet, M.; Ferrari, F. *Biotechnol. Prog.* **1990**, *6*, 198.

domain that alternated with nine GlyAlaGlyAlaGlySer repeating units.[7c] In addition, Capello and co-workers genetically expressed sequences from *B. mori* silk with those from elastin to produce block copolymers of well-defined sequences.[7d] We have recently reported silk-inspired polymers made by a novel chemical Lego method that involves catenation of preformed building blocks of defined structure and function.[8] This method is not limited to naturally occurring amino acid sequences and can handle a variety of synthetic polymer segments. It, therefore, offers the opportunity for generation of a library of protein-inspired polymers in which some but not all of the amino acid segments are replaced with synthetic nonnative segments. These can be used to provide the structure−property correlation data needed for a rational control of the properties of targeted bioinspired materials.

A key element in silk structure is self-assembled antiparallel β-sheets that form temporary cross-links and are an important factor affecting the useful properties of silk.[3c,6] In our view, β-sheet-forming polypeptides, because of their natural tendency to readily aggregate,[8,9] constitute excellent building blocks for self-assembled nanostructures. This has recently been realized in our laboratories where we found that a bioinspired synthetic material, containing poly(ethylene glycol) (PEG) soft segments that alternated with the $(AlaGly)_2$ hard segment, formed nanostructures through self-assembly of the $(AlaGly)_2$ β-sheet peptide and exhibited the solid-state properties of *B. mori* silk and $(AlaGly)_n$ in their silk II form.[8c] This has inspired us to take advantage of the natural tendency of β-sheets to self-assemble into nanostructures in delineating the factors important in nanostructure formation, which ultimately could lead to the design and synthesis of polymers of controlled architecture. Pursuant to this objective, we selected spider silk as the biopolymer to mimic.

As indicated above and revealed by the partial amino acid sequence of the spider silk structure depicted in Figure 1a, silk protein is an example of a naturally occurring segmented multiblock copolymer containing alternating poly(alanine) segments and blocks of other randomly linked amino acids. The average number of Ala residues in spider silk structures varies from 4 to 9.[6b,10] This is in the range where the poly(alanine) forms β-sheets rather than helices.[11a] Our strategy in obtaining a material whose segmented structure approximates, as closely as possible, that of silk involves replacing the segments presumed to be in the amorphous domain of silk (non-highlighted sequences in Figure 1a) with a synthetic nonpeptide segment while retaining the poly(alanine) segments (highlighted sequences). The resulting hybrid silk-mimic structures suitable for investigating nanostructure formation via β-sheet self-assembly are shown in Figure 1b. In the spider silk-inspired materials **P2** and **P3**, the poly(alanine) blocks have variable chain lengths and, therefore, can be synthesized via standard polymerization techniques, such as anionic ring-opening polymerization of the *N*-carboxyanhydride (NCA) derivative of the amino acid. The *B. mori* silk-inspired polymer **P1** has been reported previously.[8c] PEG is selected as the nonnative equivalence of the amorphous polypeptide domain because of its ready availability, ease of synthesis, well-established properties, water-solubility, biocompatibility, and controllable amorphous and crystalline character. In the above design, the lengths of the PEG segments are deliberately kept short to prevent unwanted crystallization of the PEG block and maintain the amorphous domain. Similar to **P1**, **P2** and **P3** can be readily synthesized using the reported modular synthetic approach.[8]

This paper describes the synthesis and solid-state properties of **P2** and **P3** based upon the above biomimetic design principles, discusses the relative propensity of **P2** and **P3** to self-assemble into nanostructures, and examines how the properties of natural silks are affected by the substitution of PEG for their amorphous peptide segments. Evidence for self-assembly of these materials into β-sheet nanostructures was obtained from solid-state ^{13}C NMR, solid-state FTIR, X-ray diffraction, atomic force microscopy (AFM), and differential scanning calorimetry (DSC). The paper provides evidence that rationally designed biomimetic polymers can emulate properties of the corresponding native biopolymers. It further establishes the validity of the chemical modular approach to synthesis of novel biomolecular materials of controlled architecture whose study could lead to identifying useful structure−property correlation in biomaterials.

Results and Discussion

Synthesis. The average number of Ala residues in *N. clavipes* silk (4 to 9) is readily accessible via anionic ring-opening polymerization of the NCA derivative of the amino acid. The degree of polymerization (DP) can be readily controlled by the molar ratio of the NCA to the initiator, which is typically a Lewis base. Thus, anionic ring-opening polymerization of Ala-NCA (**2**) using α,ω-diamino-PEG (**1**) as initiator gave the triblock material, poly(alanine-*b*-oxyethylene-*b*-alanine), in excellent yield (**3**, Scheme 1). The product was fractionated into water-soluble (**4**) and water-insoluble (**5**) components. End-group titration of **4** and **5** gave number average molecular weights (M_n's) as 823 and 1097, respectively. These correspond, respectively, to approximately 8 and 12 Ala residues, which are equivalent to an average DP of 4 and 6 for each poly(alanine) block. The results were confirmed by ESIMS analyses, which gave bell-shaped molecular weight profiles for each. Thus, the number of Ala residues in **4** was found by ESIMS to be 4−11, with peaks of highest intensity being DP = 7 (100%) and 8 (93%). Similarly, the number of alanine residues in **5** was found to be 7−14, with peaks of highest intensity being DP = 9 (95%) and 10 (100%).

Polymers **P2** and **P3** were prepared by step-growth polymerization of **4** and **5**, respectively, with the commercially

(8) (a) Winningham, M. J.; Sogah, D. Y. *Macromolecules* **1997**, *30*, 862−876. (b) Rathore, O.; Winningham, M. J.; Sogah, D. Y. *J. Polym. Sci., Part A: Polym. Chem.* **2000**, *38*, 352−366. (c) Rathore, O.; Sogah, D. Y. *Macromolecules* **2001**, *34*, 1477−1486. (d) Sogah, D. Y.; Claussen, R. C.; Winningham, M. J.; Rathore, O. *Ann. Technol. Conf.−Soc. Plast. Eng.* **1999**, 2180−2184. (e) Claussen, R. C.; Sogah, D. Y. *Polym. Prepr. (Am. Chem. Soc., Div. Polym. Chem.)* **1996**, *37*, 394−395. (f) Claussen, R. C. Ph.D. Thesis, Cornell University, 1998. (g) Winningham, M. J. Ph.D. Thesis, Cornell University, 1997.

(9) (a) Lashuel, H. A.; LaBrenz, S. R.; Woo, L.; Serpell, L. C.; Kelly, J. W. *J. Am. Chem. Soc.* **2000**, *122*, 5262−5277. (b) Qu, Y.; Payne, S. C.; Apkarian, R. P.; Conticello, V. P. *J. Am. Chem. Soc.* **2000**, *122*, 5014−5015. (c) Burkoth, T. S.; Benzinger, T. L. S.; Urban, V.; Lynn, D. G.; Meredith, S. C.; Thiyagarajan, P. *J. Am. Chem. Soc.* **1999**, *121*, 7429−7430. (d) Clark, T. D.; Buriak, J. M.; Kobayashi, K.; Isler, M. P.; McRee, D. E.; Ghadiri, M. R. *J. Am. Chem. Soc.* **1998**, *120*, 8949−8962. (e) Moser, R.; Klauser, S.; Leist, T.; Langen, H.; Epprecht, T.; Gutte, B. *Angew. Chem., Int. Ed. Engl.* **1985**, *24*, 719. (f) Yang, Y.; Erickson, B. W. *Protein Sci.* **1994**, *3*, 1069. (g) Kobayashi, K.; Yonezawa, N.; Katakai, R. *Macromolecules* **1995**, *28*, 8242. (h) Minor, D. L., Jr.; Kim, P. S. *Nature* **1994**, *371*, 264. (i) Gardner, R. R.; Liang, G.-B.; Gellman, S. H. *J. Am. Chem. Soc.* **1995**, *117*, 3280. (j) Schneider, J. P.; Kelly, J. W. *J. Am. Chem. Soc.* **1995**, *117*, 2533. (k) Brandmeier, V.; Sauer, W. H. B.; Feigel, M. *Helv. Chim. Acta* **1994**, *77*, 70. (l) Kemp, D. S.; Stites, N. E. *Tetrahedron Lett.* **1988**, *29*, 5057. (m) Winningham, M. J.; Sogah, D. Y. *J. Am. Chem. Soc.* **1994**, *116*, 11173.

(10) Simmons, A. H.; Michal, C. A.; Jelinski, L. W. *Science* **1996**, *271*, 84−87.

(11) (a) Fujie, A.; Komoto, T.; Oya, M.; Kawai, T. *Makromol. Chem.* **1973**, *169*, 301−321. (b) Arnott, S.; Dover: S. D.; Elliott, A. *J. Mol. Biol.* **1967**, *30*, 201−208.

Scheme 1

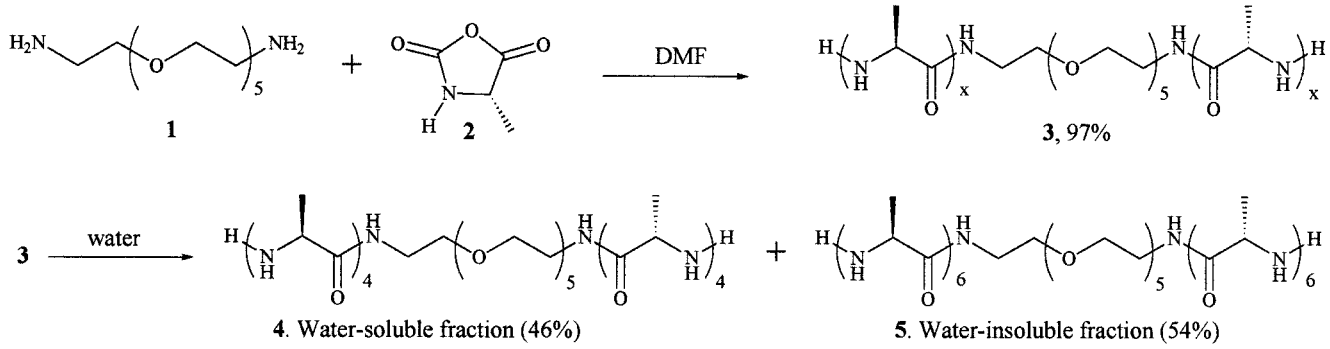

Scheme 2

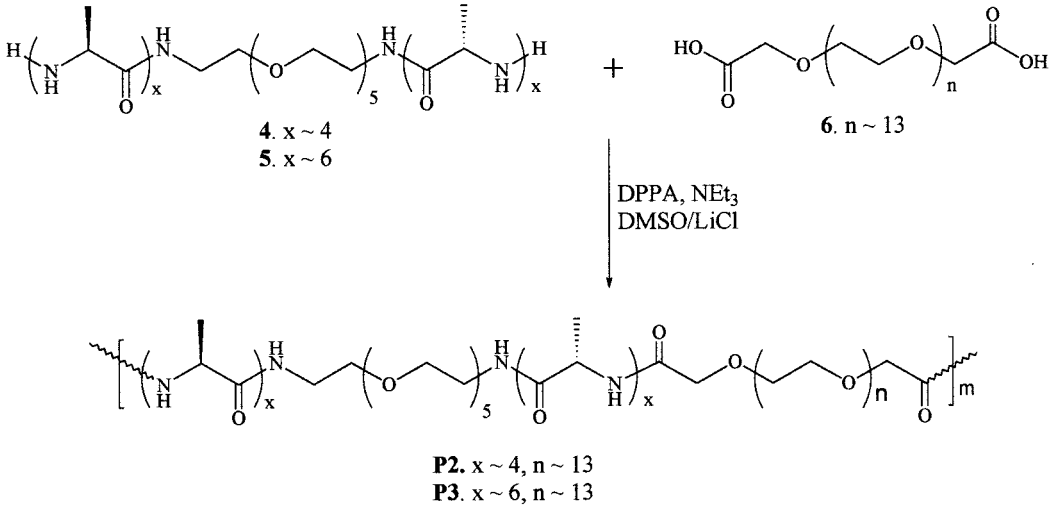

Table 1. Synthesis and Properties of Polyamides **P2** and **P3**

polymer	[Mon] (M)	yield (%)	η_{inh}[a]	T_g (°C) (DSC)[b]	T_m (°C) (DSC)[b]	$T_{d,onset}$ (°C) (TGA)[b]
P2	0.061	75	0.417	−58, −28	*d*	307
P3	0.023	68	0.305	−54, −18	*d*	337
P1[c]	*c*	*c*	*c*	−57, 0	116	300

[a] Inherent viscosity was measured in dichloroacetic acid at 25.0 ± 0.1 °C. [b] DSC and TGA were performed at 10 °C per min and 20 °C per min, respectively, under nitrogen atmosphere. [c] Reference 8c. [d] None observed.

available poly(ethylene glycol) bis(carboxymethyl) ether (**6**) as the chain extender in LiCl/DMSO and in the presence of DPPA/Et_3N (Scheme 2, Table 1).[8c] The isolated **P2** and **P3** were relatively insoluble even in a LiCl/DMSO mixture; therefore inherent viscosity (η_{inh}) measurements in dichloroacetic acid were used to obtain information about their molecular weights. The η_{inh} values of 0.42 dL·g^{-1} for **P2** and 0.31 dL·g^{-1} for **P3** correspond to weight average molecular weights (M_w's) of ca. 20000−25000 and ca. 15000−20000, respectively, based upon similar measurements reported earlier.[8a−c]

Nanostructure Formation. 1. Solid-State ^{13}C NMR Spectroscopic Evidence for the Presence of β-Sheets. Prior studies have revealed that the extent of self-assembly into nanostructures in silk-inspired materials correlated with their β-sheet contents.[8b,c] Therefore, it is important to provide unambiguous evidence that the incorporated poly(alanine) segments formed the expected β-sheets. Solid-state ^{13}C NMR[8b,c,12,13] and solid-state FTIR[8,14,15] have been shown to be effective analytical tools for demonstrating formation of β-sheets in polypeptides and proteins. Figure 2 depicts the solid-state ^{13}C NMR spectra of **P2** and **P3**. The broad resonance at 22 ppm in the Ala-C$^\beta$ spectral region (14−24 ppm) of each polymer and the resonance at 49.5 ppm (Ala-C$^\alpha$) were attributed to β-sheet aggregates. Furthermore, there was no noticeable shoulder either downfield (51−52 ppm) to the Ala-C$^\alpha$ peak or upfield (15−19 ppm) to Ala-C$^\beta$ peak in the spectra of both polymers, suggesting that **P2** and **P3** did not form significant amounts of other major non-β-sheet conforma-

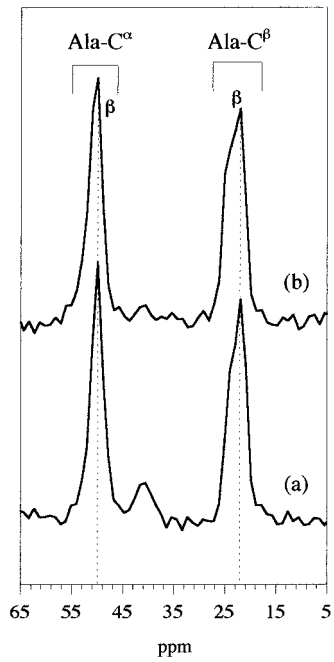

Figure 2. The Ala-C$^\alpha$ and Ala-C$^\beta$ region in the solid-state ^{13}C NMR spectra of (a) **P2** and (b) **P3**.

tions. The total β-sheet content in each polymer was estimated to be 95 ± 5%, which is comparable to that found for the structurally similar **P1** (90%)[8c] but higher than that reported for native *N. clavipes* silk (77%).[13a] The results are evidence that the predominant conformation of the poly(alanine) segments in both **P2** and **P3** is, indeed, a β-sheet. The absence of other non-β conformations, such as a helix, is in agreement with the solid-state ^{13}C NMR results of Saito et al., which revealed that a poly(alanine) with less than 16 Ala residues was more likely to form a β-sheet than a helix.[12d] Moreover, Saito et al. also did not observe significant formation of non-β conformations in poly(alanine) having greater than 4 Ala residues.[12d]

2. Evidence from Solid-State FTIR and X-ray Diffraction. The manner in which the peptides are linked to the PEG segments in the generic structures shown in Figure 1b is head-to-head and tail-to-tail. This raises the question as to whether the chain could bend onto itself to form parallel β-sheets. It was previously shown that the manner of linking say $(AlaGly)_2$ to PEG did not affect the tendency of the peptide to self-assemble into antiparallel β-sheet aggregates,[8b,c] and that formation of parallel β-sheets through intramolecular hydrogen bonding in peptides linked by flexible linear chains was entropically prohibited.[8a] Nevertheless, due to the strong tendency exhibited by **P2** and **P3** to form almost exclusively β-sheets as revealed by the ^{13}C NMR studies, and the fact that $(Ala)_3$ was found to crystallize in both parallel and antiparallel β-sheet conformations,[16] it is necessary to show independently that the observed β-sheet aggregates are not a mixture of both types of β-sheets. Using solid-state ^{13}C NMR spectroscopy to unambiguously distinguish between the two types of aggregated β-sheets does not seem straightforward and, to our knowledge, has not been previously demonstrated. Therefore we resorted to solid-state FTIR spectroscopy that, in contrast, provides a means for demonstrating the formation of β-sheets as well as distinguishing between parallel and antiparallel β-sheets.[8a−d] The resolution-enhanced (Figure 3a, dotted line) and the second derivative (Figure 3b, solid line) solid-state FTIR spectrum of **P2** (polymer with shorter poly(alanine) segments) showed bands at 1630 and 1692 (shoulder) cm^{-1}. These bands have been shown to be diagnostic for antiparallel β-sheets.[8,14,15] The FTIR spectrum also revealed bands due to random (*r*, 1655 cm^{-1}) and some non-β-sheet (non-β, 1663 and 1675 cm^{-1}) conformations; but these bands were considerably weaker than the bands attributed to the corresponding antiparallel β-sheets. Furthermore, there was no evidence for the presence of parallel β-sheets, which would have given rise to a band at approximately 1645 cm^{-1} in addition to the 1630 cm^{-1} band.[15]

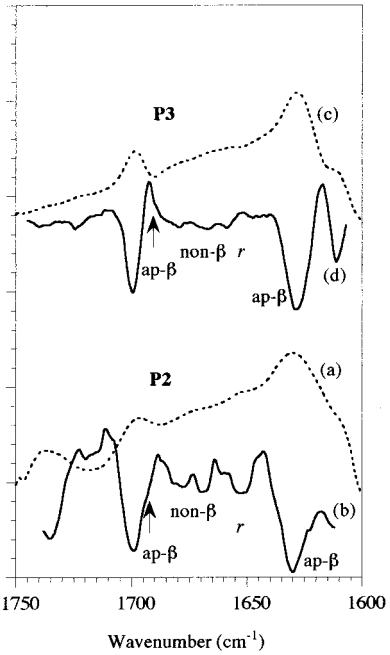

Figure 3. Solid-State FTIR spectra of **P2** and **P3** (KBr, 2.0 cm^{-1} resolution, room temperature): (a) resolution-enhanced spectrum of **P2**; (b) second derivative spectrum of **P2**; (c) resolution-enhanced spectrum of **P3**; and (d) second derivative spectrum of **P3**. (Key: ap-β, antiparallel β-sheet; *r*, random coil; non-β, non-β-sheet conformations.)

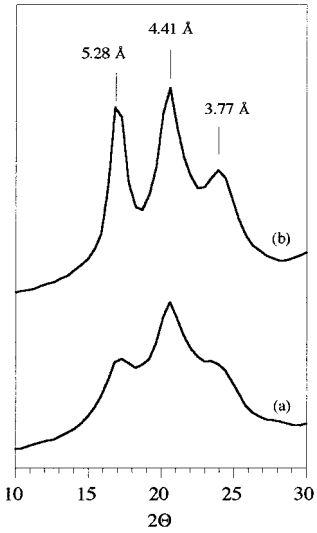

Figure 4. Powder X-ray diffraction pattern of (a) **P2** and (b) **P3**.

The relatively large band at 1700 cm^{-1} was from the amide carbonyl group of comonomer **6** fragments. The FTIR data clearly substantiate the deductions from the ^{13}C NMR studies and establish that the β-sheets are indeed antiparallel.

The formation of antiparallel β-sheets in **P2** was also confirmed by powder X-ray diffraction studies (Figure 4a). The diffraction pattern showed peaks with *d* spacings of 5.28, 4.41, and 3.77 Å. These are similar to the antiparallel β-sheet *d* spacings reported for *N. clavipes* silk by Thiel et al.[6c] and those observed for a poly(alanine) β-sheet at 5.36 and 4.45 Å corresponding, respectively, to 020 and 100 reflections in an orthorhombic crystal with $a = 4.73$ Å, $b = 10.54$ Å, and $c = 6.89$ Å.[11] To determine if the chains were aligned in any manner, X-ray diffraction studies were carried out on fibers made from **P2**. The fiber X-ray diffraction (Figure 5a) of the fibers gave arcs perpendicular the fiber axis rather than concentric circles,

(12) (a) Wishart, D. S.; Sykes, B. D. *J. Biomol. NMR* **1994**, *4*, 171−80. (b) Saito, H. *Magn. Reson. Chem.* **1986**, *24*, 835−852. (c) Saito, H.; Tabeta, R.; Asakura, T.; Iwanaga, Y.; Shoji, A.; Ozaki, T.; Ando, I. *Macromolecules* **1984**, *17*, 1405−1412. (d) Saito, H.; Tabeta, R.; Shoji, A.; Ozaki, T.; Ando, I. *Macromolecules* **1983**, *16*, 1050−1057.

(13) (a) Seidel, A.; Liivak, O.; Calve, S.; Adaska, J.; Ji, G.; Yang, Z.; Grubb, D.; Zax, D. B.; Jelinski, L. W. *Macromolecules* **2000**, *33*, 775−780. (b) Seidel, A.; Liivak, O.; Jelinski, L. W. *Macromolecules* **1998**, *31*, 6733−6736. (c) Liivak, O.; Blye, A.; Shah, N.; Jelinski, L. W. *Macromolecules* **1998**, *31*, 2947−2951.

(14) (a) Holloway, P. W.; Mantsch, H. H. *Biochemistry* **1989**, *28*, 931−935. (b) Casal, H. L.; Koehler, U.; Mantsch, H. H. *Biochim. Biophys. Acta* **1988**, *957*, 11−20.

(15) (a) Haris, P. I.; Chapman, D. *Biopolymers* **1995**, *37*, 251−263. (b) Torii, H.; Tasumi, M. *J. Chem. Phys.* **1992**, *96*, 3379−3387. (c) Surewicz, W. K.; Mantsch, H. H. *Biochim. Biophys. Acta* **1988**, *952*, 115−130. (d) Bandekar, J.; Krimm, S. *Biopolymers* **1988**, *27*, 885−908. (e) Bandekar, J.; Krimm, S. *Biopolymers* **1988**, *27*, 909−21. (f) Susi, H.; Byler, D. M. *Arch. Biochem. Biophys.* **1987**, *258*, 465−9.

(16) (a) Hempel, A.; Camerman, N.; Camerman, A. *Biopolymers* **1991**, *31*, 187−192. (b) Qian, W.; Bandekar, J.; Krimm, S. *Biopolymers* **1991**, *31*, 193-210.

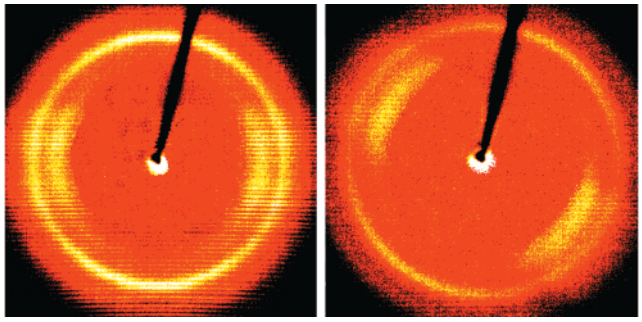

Figure 5. WAXD patterns of (a) the as-spun **P2** fiber bundle (fiber axis is vertical) and (b) the as-spun **P3** fiber bundle (the fiber axis is ~35° clockwise from vertical).

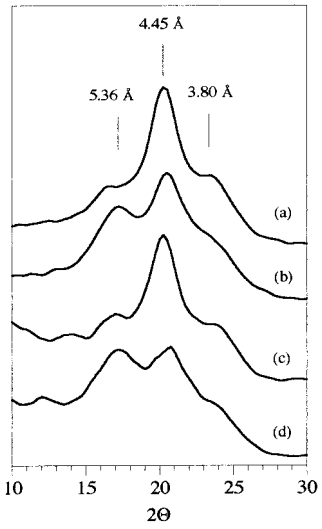

Figure 6. Radial intensity integration along (a) the **P2** fiber axis ±45°, (b) the **P2** equatorial axis ±45°, (c) the **P3** fiber axis ±45°, and (d) the **P3** equatorial axis ±45°.

suggesting that the polymer chains were aligned relatively well parallel to the fiber axis. This was confirmed by integrating the relative intensities along the fiber (Figures 6a) and equatorial (Figure 6b) axes. The *d* spacings of 4.45 and 5.36 Å were assigned respectively to the interchain spacing within a hydrogen-bonded sheet and the intersheet spacing in a poly(alanine) β-sheet.[11] The diffraction pattern is quite similar to the one observed for doubly drawn fibers of regenerated spider silk reported by Jelinski and co-workers.[13a] Hence, the solid-state FTIR and X-ray diffraction results provide conclusive evidence that the poly(alanine) segments in **P2** predominantly self-assemble into antiparallel β-sheet-containing nanostructures and that the crystalline structure is the same as that independently determined for an isolated poly(alanine).[11]

Figure 3c,d shows the FTIR spectrum of the polymer containing the longer poly(alanine) segments (**P3**). The second derivative plot (Figure 3d) revealed that this polymer also formed predominantly antiparallel β-sheet stacks as evidenced by peaks at 1628 and 1690 (shoulder) cm^{-1}. The spectrum was almost completely devoid of any evidence for other non-β conformations, which is in complete agreement with the ^{13}C NMR results (Figure 2b). Further confirmation was obtained from powder X-ray diffraction analysis (Figure 4b), which gave enhanced peak intensities at 5.28, 4.41, and 3.77 Å. As can clearly be discerned from the spectrum, the peak at 5.28 Å, which denotes intersheet spacing in poly(alanine) β-sheets, is resolved better for **P3** than for **P2**, which is consistent with its enhanced conformational purity.

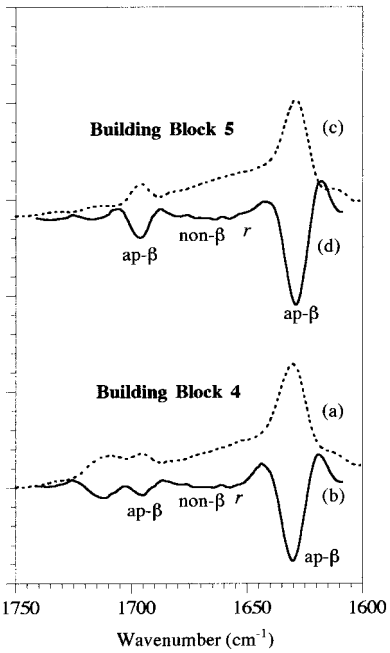

Figure 7. Solid-State FTIR spectra of building blocks **4** and **5** (KBr, 2.0 cm^{-1} resolution, room temperature): (a) resolution-enhanced spectrum of **4**; (b) second-derivative spectrum of **4**; (c) resolution-enhanced spectrum of **5**; and (d) second-derivative spectrum of **5**. (Key: ap-β, antiparallel β-sheet; *r*, random coil; non-β, non-β-sheet conformations.)

Figure 5b depicts X-ray diffraction analysis of **P3** fibers. As was the case with **P2**, **P3** polymer chains were fairly well aligned parallel to the fiber axis, which resulted in enhanced intensity of the peak at 5.36 Å integrated along the equatorial axis (Figure 6d). These observations suggest that (1) the β-sheets in both polymer chains could be aligned and oriented through fiber spinning, (2) the polymer with the higher β-sheet and lower random conformation contents exhibits higher structural order, and (3), as-made, the polymer containing the longer poly(alanine) segment has the higher propensity to self-assemble into ordered β-sheet domains. That **P2** contained more non-β conformations than **P3** might be due to the fact that **P2** contained some poly(alanine) blocks with DP < 4 (a consequence of the polymerization method used) that might not be long enough to form ordered stable β-sheets.[11a] This finding is in agreement with the results of Saito et al.,[12d] and suggests that for materials having relatively small amounts of non-β conformations, solid-state FTIR and powder X-ray diffraction are more sensitive to the nuances of nanostructure formation than solid-state ^{13}C NMR.

To determine the extent to which the structures of **P2** and **P3** are influenced by their respective building blocks, we examined the FITR spectra of **4** and **5** (Figure 7). Clearly, the solid-state structures of both building blocks are also dominated by antiparallel β-sheets as evidenced by the diagnostic bands at 1630 and 1695 cm^{-1} and the fact that the antiparallel β-bands are more intense than non-β bands. In addition, the antiparallel β-bands of **5** are resolved better and are relatively more intense than those for **4**. These suggest that **5** contains higher antiparallel β-sheet fraction than **4**. Hence, the observed relative propensity of **P2** and **P3** to form β-sheets tracks that of their respective building blocks. The results reinforce a fundamental notion in the modular method that secondary structures incorporated in building blocks can be retained in the resulting polymers, and consequently, controlling the structure of the appropriate build-

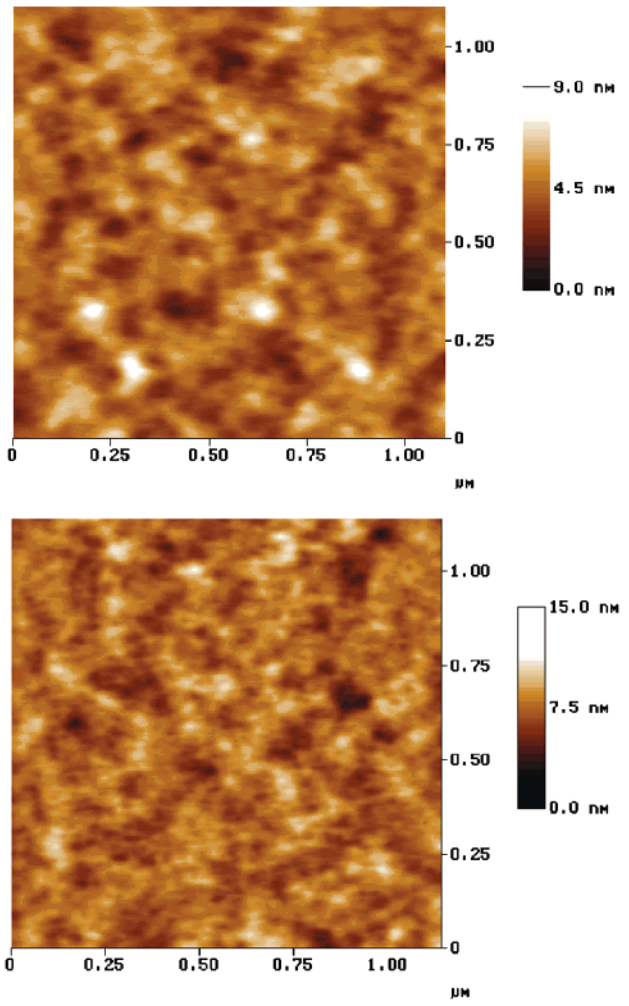

Figure 8. (a) Tapping mode AFM topological plots of (a) **P2** (top image) and (b) **P3** (bottom image) spin-coated on a silicon wafer.

ing block can lead to control of the corresponding polymer structure.

3. Evidence from AFM and DSC. The above ^{13}C NMR, FTIR, and X-ray studies provide conclusive evidence for the presence of self-assembled antiparallel β-sheets in these novel bioinspired polymers. Aggregation of the β-sheets into nanodomains would lead to hard (semi)crystalline polypeptide domains that are phase-separated from the soft PEG domains. AFM, especially in the tapping mode, can distinguish between hard crystalline domains from soft amorphous ones. Hence, the morphology of **P2** and **P3** was studied using AFM in the tapping mode. Figure 8 shows the AFM topographical plots of HFIP solution-cast films of **P2** (top) and **P3** (bottom) on silicon wafers. Under the conditions used, low regions are dark-colored while the higher regions are lighter colored; the lighter the color is, the harder and, hence, the higher is the domain. Examination of the AFM images suggests that the hard semicrystalline poly(alanine) domains are topographically higher (lightest in color) because they are stiffer than the soft PEG segments.[17] Figure 8 reveals a microphase-separated morphology containing polypeptide-rich and polyether-rich phases. In addition, larger domains (ca. 100−200 nm) are seen superimposed on the normal microphase-separated morphology with the polyether phase dispersed between them. We attribute these "superstructures" to agglomerated poly(alanine) nanostructures.[8c,18a,b] These findings are consistent with self-assembly of the poly(alanine) blocks into separate domains composed of antiparallel β-sheets. Semenov has previously suggested the existence of superstructures in polydisperse multiblock copolymers.[18a,b] He proposed that randomness in block lengths of polydisperse materials could result in two levels of organization: a microphase separation between regions with different block molecular weights superimposed on an ordinary microdomain separation. The overall morphology in Figure 8 is in qualitative agreement with the Semenov model, and is very similar to that observed by Anderson et al. for genetically engineered protein polymers based on the *B. mori* silk crystalline segment and the cell binding domains of extracellular matrix proteins coated on silicon wafers.[19] We have also previously observed such superstructures in the morphology of *B. mori* silk-inspired multiblock copolymers containing $(AlaGly)_2$.[8c] In addition, a nylon-6-based block copoly(ether amide) has been shown to exhibit the same morphology.[18c]

Table 2. Effect of Substitution on Mechanical Properties of Silk-Inspired Polymers **P1**−**P3**[a,b]

polymer	peptide segment	modulus (MPa)	tensile strength (MPa)	elongation at break (%)
P1 (film)[b]	$(AlaGly)_2$	210 ± 9	14.0 ± 0.4	21.2 ± 6.0
P2 (film)	$(Ala)_4$	308 ± 25	16.7 ± 1.1	26.2 ± 3.6
P2 (fiber)	$(Ala)_4$	410 ± 35	13.0 ± 1.4	22.9 ± 13.6
P3 (film)	$(Ala)_6$	488 ± 31	18.6 ± 0.9	12.1 ± 0.9
P3 (fiber)	$(Ala)_6$	750 ± 156	14.2 ± 2.7	5.4 ± 1.7

[a] Each entry is an average of 3−5 measurements performed at a loading rate of 0.33−0.50% per s; all films were sheared at 30−60 $cm \cdot s^{-1}$. [b] Data for **P1** are from ref 8c.

That **P2** and **P3** microphase-separate is consistent with both polymers exhibiting two glass transition temperatures (T_g's) in DSC measurements. **P2** showed T_g's at −58 and −28 °C (Table 1) while **P3** had T_g's at −54 and −18 °C. The lower T_g's correspond to the polyether-rich phase and the second T_g to the peptide-rich domain. The higher T_g of the polypeptide-rich phase observed for **P3** is consistent with its longer polypeptide blocks while the lower T_g of **P2** reflects its higher segmental motion. The thermal data confirmed that PEG crystallization was completely suppressed as no T_m was observed.

Effect of Substituting PEG for Amorphous Polypeptide Segments in Spider Silk. It is clear from the results discussed so far that, to the extent that we could determine, the solid-state structures of the polymers are similar to those observed for the native as well as genetically engineered spider silks, their analogues, and poly(alanine) of various lengths. A critical issue is how other physical properties are affected by the substitution performed on the structure. To address this issue, the modulus and tensile strength of **P2** and **P3** were determined from stress−strain curves of their respective films and fibers. Table 2 summarizes the mechanical properties of the polymers. The following conclusions can be drawn from the results in Table 2: (1) Spider silk-inspired analogue **P2** that contained an average of 4 Ala residues per segment showed higher modulus, tensile strength, and elongation at break than the *B. mori* silk-inspired **P1**, which also contained 4 peptide residues (AlaGlyAlaGly). This is consistent with the fact that native spider silk has been shown to be stronger than native silkworm

(17) McLean, R. S.; Sauer, B. B. *J. Polym. Sci., Part B: Polym. Phys.* **1999**, *37*, 859−866.

(18) (a) Semenov, A. N.; Likhtman, A. E. *Macromolecules* **1998**, *31*, 9058−9071. (b) Semenov, A. N. *J. Phys. II* **1997**, *7*, 1489−1497. (c) Chung, L. Z.; Kou, D. L.; Hu, A. T.; Tsai, H. B. *J. Polym. Sci., Part A: Polym. Chem.* **1992**, *30*, 951−953.

(19) Anderson, J. P.; Nilsson, S. C.; Rajachar, R. M.; Logan, R.; Weissman, N. A.; Martin, D. C. *Mater. Res. Soc. Symp. Proc.* **1994**, *330*, 171−7.

silk.[20] (2) Increasing the average poly(alanine) block length (as in **P3**) resulted in increased modulus and tensile strength. (3) The elongation at break decreased significantly with increasing peptide sequence suggesting lower toughness for **P3**, which is a direct consequence of the increased stiffness of the hard segment.

The above mechanical properties for **P2** and **P3** films are considerably better than those recently reported for films of regenerated spider silk.[21] Even in the case of fibers, the elongation and, hence, the toughness of **P2** are comparable to those of the natural silk fibers,[20] while the modulus and tensile strength are within just an order of magnitude of those obtained for regenerated *N. clavipes* silk[13a] and an artificial spider silk analogue protein.[20] These findings are quite remarkable given the simple nature of the building blocks used to construct **P2** and **P3**, and clearly suggest that changing the nature of the building blocks can regulate the mechanical properties of these bioinspired materials.

Summary and Conclusions

We have demonstrated that the recently reported biomolecular Lego method, whereby prefabricated building blocks are catenated block by block, is a viable approach for polymer architecture and property control. By selectively replacing certain segments of a naturally occurring structural biopolymer with a judiciously selected nonnative segment while, at the same time, retaining other segments known to be critical for essential properties of the native biopolymer, a synthetic polymer with similar properties and function can be obtained. Thus, replacement of the amorphous peptide domain of a spider silk, for example, with a synthetic nonpeptide segment, such as PEG, gave *N. clavipes* silk-inspired polymers having similar solid-state structures and very good mechanical properties. The tendency of poly(alanine) having an appropriate chain length to form β-sheets and the facility with which the β-sheets aggregate have been retained in the polymers. The almost exclusive formation of β-sheets and their self-assembly into discrete nanostructures were established by a combined use of solid-state ^{13}C NMR, solid-state FTIR, powder X-ray diffraction measurements, and AFM. The resulting morphology was a microphase-separated architecture that contained irregularly shaped 100−200 nm nanodomains interspersed within the PEG phase. It can be inferred from the results that the poly(alanine) segments influence the mechanical properties of spider silk through β-sheet self-assembly into temporary cross-links. That changing $(AlaGly)_2$ in **P1** to $(Ala)_4$ in **P2** leads to significant improvement in properties reinforces the well-known notion that properties of a particular polymer can be controlled by controlling the structure and nature of its building blocks. The results reveal a particular strength of the chemical modular method in that it can handle nonpeptide blocks and, therefore, has the potential of making available a completely new class of bioinspired polymers with useful properties.

Experimental Details

Materials. Abbreviations: Ala, alanine; Gly, glycine; DPPA, diphenylphosphoryl azide; HFIP, hexafluoro-2-propanol; PEG, poly(ethylene glycol); TFE, trifluoroethanol. Common reagents were purchased from Aldrich, Sigma or Acros and solvents from Fisher Scientific or Mallinckrodt. CH_2Cl_2 was distilled from CaH_2 and stored over 3 Å molecular sieves. PCl_3 was refluxed and distilled prior to use. THF and toluene were distilled from purple Na/benzophenone solutions. DMSO was distilled from CaH_2 onto 4 Å molecular sieves. Glassware was dried in an oven and cooled under nitrogen where appropriate. Synthesis of 3,6,9,12,15-pentaoxaheptadecane-1,17-diamine (**1**)[8b] and the *N*-carboxyanhydride derivative of Ala (**2**)[22] were performed in accordance with literature procedures. **1** was further purified using Kugelrohr distillation. Instead of washing with CCl_4 as reported in the literature, the crude Ala-NCA (**2**) was recrystallized twice from THF/toluene. Poly(ethylene glycol) bis(carboxymethyl) ether (**6**, $M_n \sim 600$) was purchased from Aldrich and used without purification.

Characterization. Solution ^{1}H and ^{13}C NMR spectra were recorded on an AF-300 spectrophotometer. Solid-state ^{13}C NMR CPMAS spectra were recorded at 75.22 MHz on a "home-built" instrument. FTIR spectra were recorded on a Perkin-Elmer 16PC FTIR spectrometer. Solid-state FTIR samples were prepared as 0.3−0.5 wt % in KBr pellets, and the spectra were obtained with 50 scans at a resolution of 2.0 cm^{-1} for 1750−1600 cm^{-1}, and at 4.0 cm^{-1} from 4000 to 1000 cm^{-1}. Inherent viscosity measurements were done in DCA solutions with a Cannon-Ubbelohde C1 C866 viscometer, which was placed in a water bath thermostated at 25 ± 0.1 °C. Solubility tests of the polymers were carried out at 1 mg/mL concentration. Thermogravimetric analysis (TGA) and differential scanning calorimetry (DSC) were performed on a Seiko 5200 thermal analysis system with TGA/DTA 220 and DSC 220C units under a positive flow of nitrogen at a heating rate of 20 and 10 °C/min, respectively. Glass transition temperatures (T_g's) and melt transitions (T_m's) were recorded from the second heating cycle. Melting points were measured on an Electrothermal IA90 melting point apparatus and are uncorrected. Powder X-ray diffraction was performed on a $\theta-\theta$ Scintag diffractometer with a Cu source ($\lambda = 1.5405$ Å). X-ray diffraction data for fibers were obtained on a Bruker-Axs D8 system ($\lambda = 1.5405$ Å) with a 2-D detector at 40 kV and 40 mA. All X-ray diffraction data were smoothed for presentation without generating artifacts. Tensile measurements were performed on films and fibers using an Instron tensile testing system (series 1122) at 21 °C and 65% relative humidity. The ends of the films and fibers were immobilized onto pieces of cardboard that were then clamped during measurements. AFM samples were prepared by spin-coating a 10% (w/v) HFIP solution of the polymer on silicon wafers at 4000 rpm and immediately drying the wafer at 115 °C for 1 min in vacuo. The samples were visualized on a Nanoscope III (Digital Instruments), using a 12-μm D scanner in air, in the tapping mode. The AFM was mounted on a homemade anti-vibration table and on an isolation chamber. AFM tips from Digital Instruments with force constants of 50 N/m (manufacturer's specifications) were employed. A resonant frequency of 300 kHz was used.

Film Casting and Fiber Spinning. **P2** and **P3** films were obtained by casting onto glass slides from 40% (w/v) HFIP solutions using a micron film applicator from GARDCO. The glass slides were sprayed prior to use with Fluoroglide anti-stick agent to facilitate lift-off. The films were dried at 70−75 °C overnight in vacuo prior to testing. Continuous fibers were spun from **P2** (10−15% w/v HFIP solution) and from **P3** (5% w/v HFIP solution) by extruding the spinning dope contained in a 100 μL LuerLok syringe equipped with a needle having an internal diameter of 350 μm and a length of 8 mm. The coagulant used was methanol−acetone (1:1), and the extruded filaments were allowed to cure for 1 h in the bath prior to removal by reeling. The fibers were dried at 70−80 °C overnight in vacuo prior to testing.

3,6,9,12,15-Pentaoxaheptadecane-1,17-diamidobis[poly(alanine)] (3). To a 250-mL round-bottom flask equipped with a stirring bar was added Ala-NCA (**2**, 3.23 g, 28.06 mmol). The flask was sealed with a rubber septum and 40 mL of DMF was introduced via cannulation. The mixture was stirred until the solids dissolved after which a solution of **1** (0.655 g, 2.34 mmol) in 5 mL of DMF was added via a syringe under nitrogen. The mixture was allowed to stir at room temperature under nitrogen atmosphere for 1 day. The reaction mixture was precipitated into 400 mL of diethyl ether and filtered. The solids thus obtained were washed with absolute ethanol (3 × 30 mL) and acetone (3 × 30 mL). The resulting white powder was dried in vacuo to yield **3** (2.57 g, 97%). The product was fractionated by

(20) Jelinski, L. W. *Curr. Opin. Solid State Mater. Sci.* **1998**, *3*, 237−245.

(21) Hinman, M. B.; Jones, J. A.; Lewis, R. V. *Trends Biotechnol*. **2000**, *18*, 374−379.

(22) Akssira, M.; Boumzebra, M.; Kasmi, H.; Dahdouh, A.; Roumestant, M. L.; Viallefont, P. *Tetrahedron* **1994**, *50*, 9051−9060.

treatment with 75 mL of water. The water-insoluble material was filtered and dried in vacuo to yield **5** (1.3 g): mp 191.5−195.1 °C dec. ^{1}H NMR (300 MHz, ppm, TFA-d): δ 4.70 (m, Ala-αH), 4.51 (m, Ala-αH), 3.93 (m, $-OCH_2CH_2-$ and OCH_2CH_2NH-), 3.70 (m, $-OCH_2CH_2NH-$), 1.40−1.81 (overlapped d, Ala-βH). End-groups (by aqueous titration): 1.823 mmol/g. M_n = 1097 (by end-group analysis). ESIMS (*m*/*z*, relative intensity): 778.4, 30%; 849.4, 56%; 920.8, 95%; 991.8, 100%; 1062.6, 58%; 1133.2, 24%; 1205.2, 14%. Elemental analysis: C, 49.32; H, 8.02; N, 16.72.

The filtrate was lyophilized to obtain **4** (1.1 g): mp 186.7−189 °C dec. ^{1}H NMR (300 MHz, ppm, D_2O): δ 4.25 (m, Ala-αH), 3.86 (m, Ala-αH), 3.66 (m, $-OCH_2CH_2-$), 3.59 (collapsed dt, OCH_2CH_2NH-), 3.37 (m, $-OCH_2CH_2NH-$), 1.12−1.49 (overlapped d, Ala-βH). End-groups (by aqueous titration): 2.431 mmol/g. M_n = 823 (by end-group analysis). ESIMS (*m*/*z*, relative intensity): 565.9, 5%; 636.5, 20%; 707.5, 47%; 778.6, 100%; 849.7, 93%; 920.9, 43%; 991.7, 11%. Elemental analysis: C, 48.88; H, 7.75; N, 15.20.

Synthesis of P2 in Solution. To a dried 25-mL round-bottom flask equipped with a magnetic stirring bar and a gas-inlet adapter were added **4** (0.500 g, 1.22 mmol $-NH_2$ groups), **6** (0.424 g, 1.22 mmol −COOH groups), and 10 mL of 2.5% LiCl in DMSO. The mixture was cooled to ∼12−15 °C and NEt_3 (0.68 mL, 4.88 mmol) and DPPA (0.34 mL, 1.58 mmol) were added. The reaction was stirred rapidly at 12−15 °C for 10 min and then allowed to warm to room temperature. After 2 days the mixture was again cooled to ∼12−15 °C and NEt_3 (0.40 mL, 2.87 mmol) and DPPA (0.34 mL, 1.58 mmol) were added. The reaction was stirred at room temperature for a further 2 days. The polymerization mixture was pipetted into 400 mL of EtOAc. The crude product was washed successively with diethyl ether (3 × 50 mL), MeOH (3 × 50 mL), and diethyl ether (2 × 50 mL). The resulting off-white solid was dried in vacuo to yield **P2** (672 mg, 75%). DSC: T_{g1} −58 °C, T_{g2} −28 °C. TGA: $T_{d,onset}$ 307 °C. η_{inh} = 0.417. IR (KBr, 4.0 cm^{-1}): 3488 (sh), 3277, 3075, 2915, 1736, 1699, 1682 (sh), 1678, 1668, 1652, 1630, 1610, 1537, 1451, 1400, 1358, 1292, 1247, 1100. Elemental analysis: C, 50.89; H, 7.66; N, 9.55; P, <0.05.

Synthesis of P3 in Solution. The procedure for **P2** was followed using **5** (0.500 g, 0.912 mmol $-NH_2$ groups), **6** (0.318 g, 0.912 mmol −COOH groups), NEt_3 (0.38 mL + 0.30 mL, 2.73 mmol + 2.15 mmol), DPPA (0.26 mL + 0.26 mL, 1.21 mmol + 1.21 mmol), and 20 mL of 2.5% LiCl in DMSO to give **P3** (611 mg, 68%) as an off-white solid. DSC: T_{g1} −54 °C, T_{g2} −18 °C. TGA: $T_{d,onset}$ 337 °C. η_{inh} = 0.305. IR (KBr, 4.0 cm^{-1}): 3486 (sh), 3276, 3077, 2917, 1723, 1700, 1685 (sh), 1679, 1668, 1659, 1628, 1611, 1531, 1450, 1398, 1370, 1299, 1238, 1102. Elemental analysis: C, 50.71; H, 7.67; N, 12.08; P, <0.05.

Acknowledgment. This work was supported by the Cornell Center for Materials Research (CCMR), a Materials Research Science and Engineering Center of the National Science Foundation (DMR-9632275, DMR-0079992). The authors are grateful to Dr. D-K. Yang for assistance with ^{13}C NMR experiments, Dr. M. Weathers for assistance with X-ray diffraction, and D. J. Diaz for assistance with atomic force microscopy.

JA004030D